Implementation of Sensorless Field Oriented Control Algorithm for Variable-Speed Rotary Compressors Using Digital Signal Controller

Fatih E. Uzun[1], Koray Gürkan[1], Tugay Bozik[2], Sergen E. Arslan[2], Umut Güven[2], Sıddık Yarman[1]

[1] Department of Electrical and Electronics Engineering, Istanbul University, Avcilar, Istanbul, Turkey
kgurkan@istanbul.edu.tr
[2] Tumble Dryer Plant, Arcelik A.S., Cerkezkoy, Tekirdag, Turkey
sergenerkan.arslan@arcelik.com

Abstract

In this paper, a variable-speed rotary compressor controller was developed by using low-cost high performance digital signal controller. Sensorless control of compressor's interior permanent magnet synchronous motor is obtained using fundamental excitation method. Start-up, rotor alignment, merging, position and speed estimation algorithm was explained. Developed system was tested with a loaded rotary compressor that is the part of a heat-pump system and experimental results were presented.

1. Introduction

A compressor is used to compress a working fluid (i.e., the refrigerant) from initial (suction) conditions to compressed (discharge) conditions. It is used in a wide variety of industrial and residential applications to circulate refrigerant to provide a desired heating and/or cooling effect with high energy efficiency. The method of using the heat from a condenser of vapor compression cycle is known as heat pump. Heat pumps have Coefficient of Performance (COP), which is the ratio of heating capacity to electrical power consumption, in the range of 2 to 4 and a corresponding Seasonal Energy Efficiency Ratio (SEER) of 9 to 13 [1]. The variable speed units based on variable speed capacity controlled compressors became standard in heat pumps as the "efficiency" has become an important issue for the industry. The application of inverter technology in air conditioning systems for commercial and residential purposes was first implemented in Japan in 1980s. Since then, these systems have become popular owing to their energy saving and better maintaining of thermal comfort when compared to the constant speed operation [2]. In units with a variable-speed compressor, or inverter, the refrigerant cycle operates at different speeds depending on temperature and heating loads. By automatically adjusting the speed of the refrigerant, the inverter eliminates energy losses caused by stopping and starting. The energy savings in the range of 10-25%, compared to fixed speed On/Off controlled heat pumps [3].

There are basically two types of compressors that are commonly used in the heat-pump industry, that is, reciprocating and rotary. Rotary compressors compresses the refrigerant gas by a rotating mechanism. Reciprocating compressor does the same by converting a rotating action of a motor into a linear action. In comparison to reciprocating compressors, rotary compressors offer a reasonable balance between initial cost, maintenance, efficiency, size and options.

Rotary compressors are commonly includes a permanent-magnet synchronous motor (PMSM) that provides suction and compression force. In these machines efficient speed and torque control requires a simultaneous control of several variables. Sensorless control of PMSMs has been extensively investigated and reported in many literatures, because elimination of speed sensor provides the advantages of reduced cost and size, higher reliability and less maintenance requirements. Under light or slowly varying load conditions open-loop speed control of PMSM is possible [4]. However, for rotary compressors, closed-loop control is necessary for correct operation as suction and compression load is heavy and instantly changing [5, 6]. Especially, Field oriented control (FOC) of PMSM can decouple its torque control from field control which allows the induction motor to act like a separately excited DC motor [7].

The PMSM sensorless control approaches proposed in the literature are mainly classified into two strategies: the fundamental excitation (model-based) and saliency and signal injection (unmodel-based). The first is based on state observers like back-electromotive force (back-EMF), sliding mode (SMO), extended Kalman Filter (EKF) techniques for position estimation measuring only fundamental excitation variables such as stator voltages and currents. These methods offer accurate position estimation when PMSM is operating in the middle and high-speed range [8]. Signal injection strategy is suitable for low-speed and standstill running condition of PMSM [9].

Because of the requirements of fast computation, programmable ability, embedding processor, low power consumption, hardware/software co-design etc. an optimum solution is necessary for realization of compressor control, because installation of an expensive control unit into an air-conditioner, refrigerator or into tumble-dryer is not practical. In literature, several practical implementations based on FPGAs [10-12], DSPs [13-15] are presented. Digital signal controllers (DSC) are also very well suited in applications where efficiency, high performance, and cost are key requirements. In this study a DSC based sensorless control algorithm implemented and tested for variable speed rotary compressors.

2. Sensorless Control Theory

A state observer based on sensorless control strategy is a good solution for a wide range of low cost applications. In this observer the complete motor model is used to estimate the whole state variable which include both the unknown rotor speed and position and the measurable motor currents. The observer needs relative accuracy in the modeling of the equation

of the unknown variables, the measurements of the motor currents, and the knowledge of the supply voltages. The position estimation scheme used here is a current-model-based algorithm, in which the motor currents are estimated in a hypothetical plane using the voltage equations of the PMSM, an estimated position error is obtained from the errors between the estimated and measured currents, and the rotor speed and position are calculated from the estimated position error. In Fig.1, the α–β and d–q frames represent the stationary and the rotor reference frames, respectively. The α-axis corresponds to the magnetic axis of the a-phase and the d-axis is aligned with the direction of the north pole of the rotor. The γ–δ frame is an estimated frame used in the sensorless vector control, and θr is the actual rotor position [16]. These frames can be obtained by well-known Clarke and Park transformations.

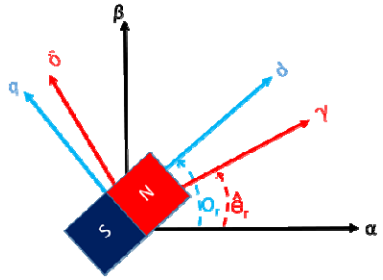

Fig. 1. Space vector diagram of PMSM

By assuming that position estimation is nearly zero, the voltage equation for the PMSM in the γ–δ frame is given by;

$$\begin{bmatrix} u_d \\ u_q \end{bmatrix} = \begin{bmatrix} R + sL_d & -wL_q \\ wL_d & R + sL_q \end{bmatrix} \begin{bmatrix} i_d \\ i_q \end{bmatrix} + \begin{bmatrix} 0 \\ w\psi_s \end{bmatrix} \qquad (1)$$

where u_d and u_q are the γ–δ axis stator voltages, i_d and i_q are the γ–δ axis stator currents, R is the stator resistance, L_d and L_q are the d–q axis stator inductances, ψ_s is the permanent magnet flux linkage, s is the differential operator, ω is the electrical angular velocity of the rotor. The FOC control method is often applied to PMSM motors with a sinusoidal back-EMF waveform shape to achieve high torque performance and efficiency.

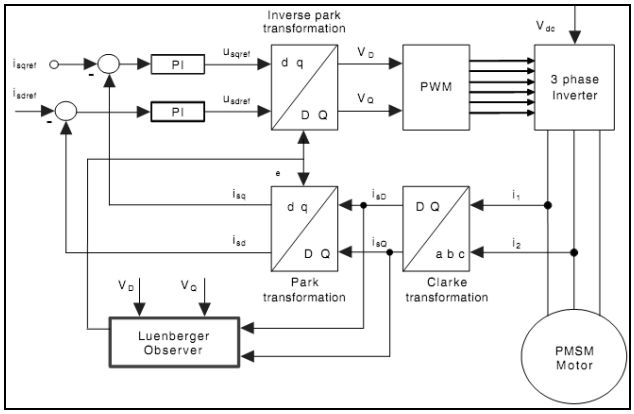

Fig. 2. Sensorless control scheme

The Luenberger observer can be used to detect the instantaneous value of the two motor back-EMF components, in the stator frame, of PMSM needed to identify the rotor position. It is ensures stability and convergence of the observer even when the system being observed is unstable. Fig. 2 shows the block diagram of the FOC control: the two motor phase currents, (i_{s1},i_{s2}), are measured with two current sensors and then the 2 currents are projected with Clarke transformation in the stator frame D, Q. Outputs of this block are the two current components (i_{sD}, i_{sQ}) in the D, Q stator fixed frame. i_{sD} and i_{sQ} are used inside the Luenberger observer together with v_D v_Q; the output is cos(theta) sin(theta) used for Park transformations. These current components are also used as inputs of the park transformation module that gives as output the current components (isd, isq) in the d, q rotating reference frame. i_{sd} and i_{sq} measured current components are compared to the references isdref (the flux reference) and i_{sqref} (the torque reference) and corrected by mean of two PI controllers. Then the outputs of two PI, u_{sd} and u_{sq}, are sent to the Inverse Park transformation module from which we get the new components of the stator voltage vector in the (u_{sD}, u_{sQ}) non-rotating stator frame. These signals are then appropriately processed to produce voltage signals for the output bridge. In our case, it is chosen to use the space vector modulation (SVM) technique to impress the new voltage vector to the motor [4].

3. Digital Signal Controller

The computation time of the controller must be low enough to provide a seamless drive even at high speeds. In this study, a low-cost DSC (MC56F84550) is used based on 32-bit 56800EX core with up to 80 MIPS at 80 MHz core frequency and DSP-MCU functionality in a unified, C-efficient architecture. It includes two high-speed, 8-channel, 12-bit ADCs with dynamic x2, x4 programmable amplifier, one PWM module with up to 9 PWM outputs, including 8 channels with high resolution. It has a crossbar inter module connection property which provides that PWM and ADC module can be synchronized. CodeWarrior embedded software development tool is used for code development. Manufacturer of the DSC provides useful libraries for sensorless control, however, all parameters must be fully understood by users.

4. Algorithm

We can split sensorless PMSM motor control algorithm into 4 steps; align, open-loop start-up, transition & merging, FOC current control, respectively.

4.1 Align

At the beginning of application all of the parameters about motor and motor control are sent to the main structure of the PMSM algorithm. Then the algorithm starts with the Align process. Align algorithm block is shown in Fig. 3. The proposed align algorithm works as follows; first, for a period of t time which is determined empirically, D voltage and θ_1 position is applied to the inverse park transformation. Then, for the rest of the same D voltage and θ2 positon is applied to the inverse park transformation. During this process Q voltage is always kept at zero.

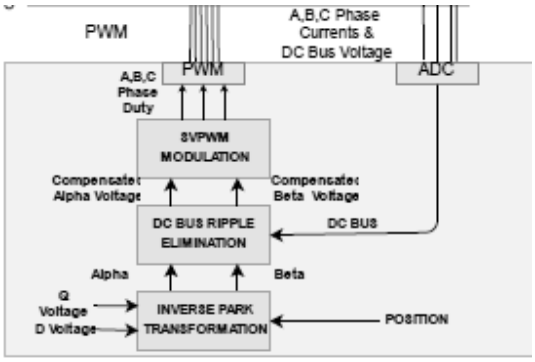

Fig. 3. Align algorithm components

With this operation we assume that the rotor of the PMSM motor moved from positon θ_1 to θ_2. After that we take the start point of the SVPWM (Space Vector Pulse Width Modulation) as θ_2. All of these variables (t, θ_1, θ_2, D voltage) can variate for different applications. The parameters we used for this application is given in Table 1.

Table 1. Align Parameters

D (Volt)	120
θ_1 (Degree)	240
θ_2 (Degree)	0
T (ms)	400

4.2 Open-Loop Startup

After the alignment process, program moves to the second step. The main objective of startup process is to accelerate the PMSM motor to a certain speed value. This speed values is called catch-up speed and it variates depending to the PMSM motor used in applications. There is 3 important part of the Open-Loop Start-Up process these are the current sense algorithm, integrator coefficient, and start-up Q current, I_q.

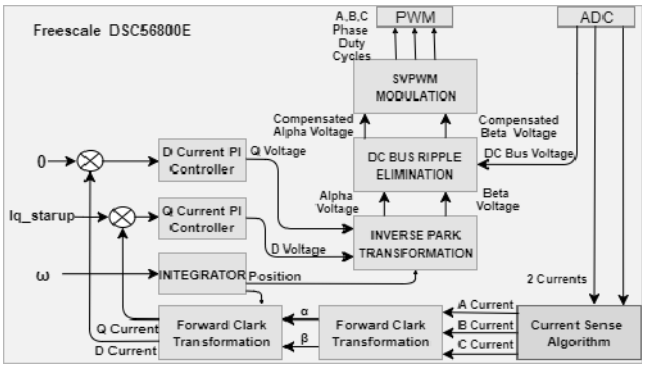

Fig. 4. Open-Loop start up algorithm

As mentioned earlier MC56F84550 has a crossbar inter module which provides that PWM and ADC module can be synchronized. Also MC56F84550 has 2 ADC modules and they be used parallel to take 2 ADC samples at the same time. The ability to take 2 ADC samples at the same time is crucial for the motor control applications. But since the motor driving technique is SVPWM the 2 ADC sample is changes according to the SVPWM state. According to the [17] ADC sample always needs to be choose according to the PWM duty cycles of the low levels of H-bridge. For example if the highest low level duty cycles belongs to phase A and phase B, microcontroller's ADC status registers programed to take sample from A and B phases. This current sense technique increases the current sensibility at low currents.

At the open loop start up, motor speed comes from the ramp function which is in the slow-loop. The compressor used on this project has a ramp values of 60 RPM/sec. Then speed value goes to the integrator function to derive the motor position. The integrator gain is very important for the sensibility of the position.

Start-up Q current value must be high enough to move the motor at the start. Therefore mostly at the beginning this value is taken the highest current that can be used. Then, it is gradually decreased. But it must be still high enough to create enough current for the observer. At the low current values observer tends to behave unstably.

4.3 Transition & Merging

After motor reached the catch-up speed it can pass from open loop to close loop. The transition algorithm is given in Fig. 5. In the transition algorithm observer is activated. The detailed algorithm diagram of observer is given in Fig. 6.

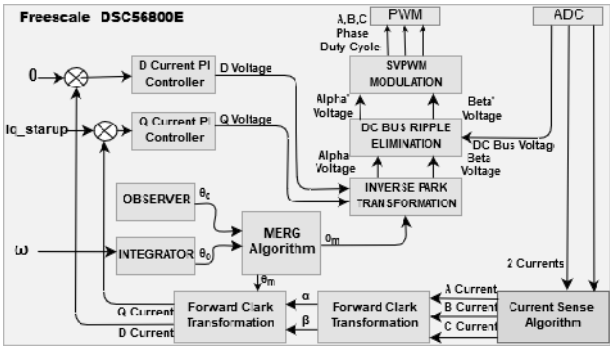

Fig. 5. Transition & Merge algorithm

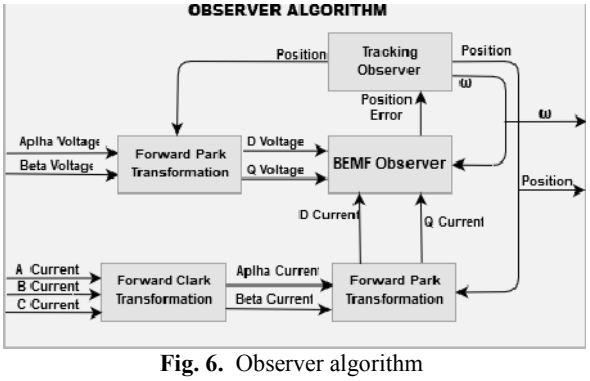

Fig. 6. Observer algorithm

There is a Forward Park (FP) transformation in the observer algorithm. Normally this function is not used and the motor D, Q voltages given directly to the BEMF observer. But in the transition part, motor D, Q voltages is created with Inverse Park transform using open loop position (θ_o) and θ_o is not equal to θ_c. That's why at the transition process D, Q feedback voltages are created by FP transformation of the Alpha Beta voltages of

the motor using the position created by observer. Also finding the right PI parameters for the tracking observer might be quite difficult. After the observer activated and observer speed matches the open loop speed with the error less than the preferred one, the merge algorithm is started. There is always an error between observer positon and the open loop positon. This error can lead to current peaks, motor mall functions or noise if it's ignored and motor positon changed in directly from open loop positon to the observer position [17]. To prevent this, merge algorithm is used. At the transition merge algorithm converges the open-loop positon to the observer positon with that the error between this positons is decreased at the transition point. The change between positon is shown in Figure 5. Because the DSC core uses normalized variables the position values shown is normalized with 180 degrees, in etc., if we take the error between positon as 0.1 at 0 sec. this value corresponds to 18 degrees. Merge algorithm is started when merge ratio is 0 and ended when the merge ratio is 1. As shown in the Fig.7 the error between positon is almost zero.

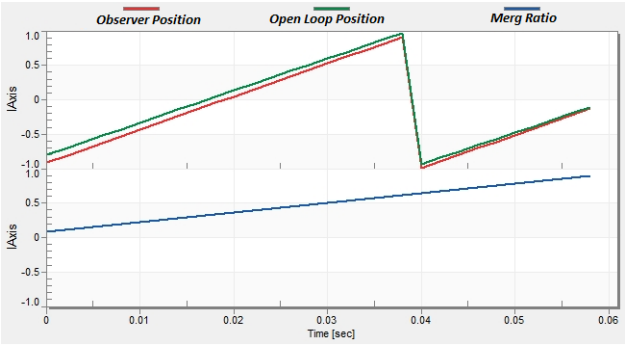

Fig. 7. Transition and merging

4.4 Field Oriented Current Control

In field oriented current control positon is obtained directly from the observer. The input value of Q Current PI is comes from the Speed PI which is inside the slow-loop (Fig. 8). Since the Speed PI is not supposed to have a fast response time it is placed inside the slow-loop. The ratio between slow-loop and fast-loop is generally taken as 10. For example if the frequency of PWM and fast-loop is 10 kHz then slow-loop frequency is taken as 1 kHz.

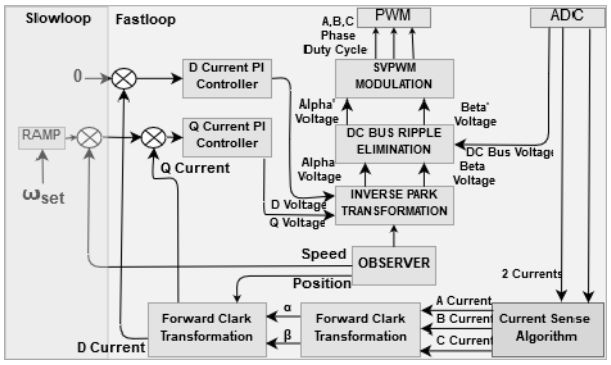

Fig. 8. FOC Current Control

5. Experiments

Experiments conducted with 4-poles 750 W rated rotary compressor. Other parameters of the compressor are summarized in Table 2. To test the working condition of the compressor, a barometer is attached to the pipeline. To drive the compressor, a tailor made inverter board is used which has a 1 kW rated power [4]. To set PI parameters more accurately and determine the energy consumption, a high-frequency power analyzer (HIOKI 3390) is used. Three current clamps are connected to the compressor's phase lines. Also to monitor the synchronization between the PWM signals and ADC sampling time, a four-channel digital oscilloscope (RIGOL MSO1104Z) is used. Inverter board is supplied with an AC power supply (KEYSIGHT AC6803) to test the behavior of the algorithm at the varying AC voltage levels and to isolate experiment set-up from the mains line (Fig. 9, Fig. 10).

Table 2. Properties of PMSM Compressor

Number of Poles	4
Rated output [W]	750
Rated torque [Nm]	0.399
Rated current [Arms]	1.75
Back-EMF Constant (Vs/krpm)	27.2

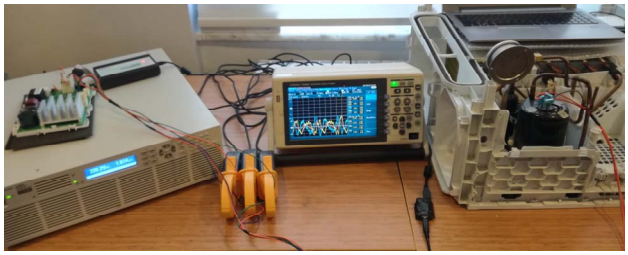

Fig. 9. Test Bench

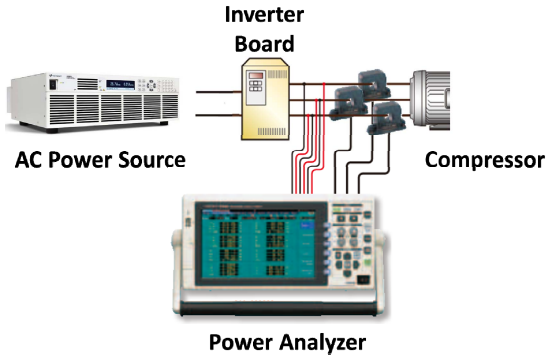

Fig. 10. Measurement set-up for testing compressor driver

AC power supply has also power measurement capability which has 1 W resolution. To visualize the condenser and evaporator temperature differences, a thermal imager (FLUKE Ti27) is used. In experiments rotation speed of compressor is varied between 2400-5000 RPM and power supply output power, compressor phase currents/voltages, and barometer pressure are measured. After each step, compressor have been shut-off and not started again, until barometer pressure was reduced to 7 bar.

Table 3. Measured values for variable-speed operation

Compressor Speed (RPM)	Supply Output Power (W)	Compressor Phase Current (A)	Compressor Phase Voltage (V)	Compressor Pressure (Bar)
0	22	0	0	7.0
2400	210	2.30	210.0	11.5
2740	260	2.40	209.3	14.0
3460	375	2.30	207.5	17.0
3700	400	2.41	207.3	18.5
4500	610	3.00	204.9	25.0
5000	750	3.17	203.04	27.0

Experiments show that below the 1000 RPM, back-EMF is not detectable and observer could not work, thus, closed-loop operation is not possible. For high speed operation, close-loop operation is essential as rotary compressor pressure gets higher. In several experiments, lockouts have occurred after closed-loop transition. Thermal image of condenser and evaporator surfaces shows that compressor is working properly (Fig.11).

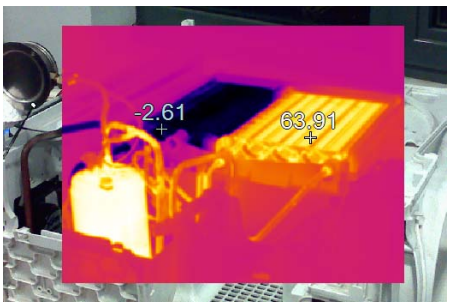

Fig. 11. Thermal image of condenser and evaporator surfaces

6. Conclusion

Variable speed rotary compressor successfully controlled by field oriented sensorless control which is conducted with low-cost MC56F84550 digital signal controller. System is fast enough to compute transformations, capable of multi-tasking operations like multi-channel ADC sampling and PWM generation. Libraries provided by manufacturer is time saving property.

7. Acknowledgment

This study is supported by the Scientific and Technological Research Council of Turkey (TUBITAK Project No: 5150011).

8. References

[1] R.S. Adhikari, N. Aste, M. Manfren, D. Marini, “Energy savings through variable speed compressor heat pump systems”, *Energy Procedia*, vol. 14, pp. 1337-1342, 2012.

[2] Ghosh, Alok, and Kundlik V. Mali. "A review on DC inverter operated air conditioner", *International Journal of Current Engineering and Technology*, Special Issue-7, 2017.

[3] S.A. Tassou, C.J. Marquand, D.R. Wilson, “Comparison of the performance of capacity controlled and conventional on/off controlled heat pumps”, *Applied Energy*, vol. 14, issue 4, pp. 241-256, 1983.

[4] A, Sergen E., et al. "Realization of SV-PWM motor control algorithm using ARM Cortex-M4 based microcontroller", *National Conference on. Electrical, Electronics and Biomedical Engineering (ELECO)*, pp. 282-285, 2016.

[5] Cho, Kwan-Yuhl., "Sensorless control for a PM synchronous motor in a single piston rotary compressor." *Journal of Power Electronics,* vol. 6, no. 1, pp. 29-37, 2006.

[6] Park, Cheon-Su, et al. "Active mechanical vibration control of rotary compressors for air-conditioning systems", *Journal of Power Electronics*, vol. 12, no. 6, pp. 1003-1010, 2013.

[7] Nisha, G. K., Z. V. Lakaparampil, and S. Ushakumari. "Torque capability improvement of sensorless FOC induction machine in field weakening for propulsion purposes", *Journal of Electrical Systems and Information Technology*, vol. 4, no.1, pp. 173-184, 2017.

[8] Ilioudis, Vasillos C., "A model based sliding mode observer applied in PMSM sensorless control for speed and position", *25th Mediterranean Conference on Control and Automation (MED)*, 2017.

[9] Kung, Ying-Shieh, et al., “Design and digital hardware implementation of a sensorless controller for PMSM drives using LF signal injection and EKF”, *International Conference on Applied System Innovation (ICASI) IEEE*, pp. 1281-1284, 2017.

[10] Kung, Ying-Shieh, et al. "*FPGA-based speed controller design for a ceiling fan motor*", IEEE 3rd International Future Energy Electronics Conference and ECCE Asia (IFEEC 2017-ECCE Asia), 2017.

[11] Chang, Yen-Chuan, and Ying-Yu Tzou. "Single-Chip FPGA Implementation of a Sensorless Speed Control IC for Permanent Magnet Synchronous Motors", *IEEE Power Electronics Specialists Conference*, (PESC), 2007.

[12] Kung, Ying-Shieh, Yi-De Lin, and Liang-Chiao Huang. "FPGA-based sensorless controller for PMSM drives using sliding mode observer and phase locked loop", *IEEE International Conference on Applied System Innovation (ICASI),* 2016.

[13] Niu, Li, et al. "A smooth and fast transition method for PMSM SMO based sensorless control", *IEEE Annual Southern. Power Electronics Conference (SPEC)*, 2016.

[14] Zhang, Yongchang, et al. "A comparative study of Luenberger observer, sliding mode observer and extended Kalman filter for sensorless vector control of induction motor drives", *IEEE Energy Conversion Congress and Exposition (ECCE),* 2009.

[15] Saadaoui, Oussama, et al. "A sliding-mode observer for high-performance sensorless control of PMSM with initial rotor position detection." *International Journal of Control* vol. 90, no. 2, pp. 377-392, 2017.

[16] K. W. Lee, S. Park and S. Jeong, "A seamless transition control of sensorless PMSM compressor drives for improving efficiency based on a dual-mode operation," *IEEE Transactions on Power Electronics*, vol. 30, no. 3, pp. 1446-1456, 2015.

[17] Freescale Semiconductor, “Sensorless PMSM Field Oriented Control”, Document Number: DRM148.

[18] Freescale Semiconductor, “Tuning 3-Phase PMSM Sensorless Control Application Using MCAT Tool”, Document Number: AN4912.